Addendum to *Blue Noise through Optimal Transport*

Fernando de Goes, Caltech
Katherine Breeden, Stanford
Victor Ostromoukhov, Lyon 1 U./CNRS
Mathieu Desbrun, Caltech

ACM Transactions on Graphics, 31(6) (SIGGRAPH Asia)

DL PDF WEB CODE

In this addendum, we provide lengthier derivations of the closed-form expressions presented in the main text, and present additional blue noise results and comparisons to previous techniques.

1 Functional and its Derivatives

Notation: A power diagram for a weighted point set $(\mathbf{X} = \{\mathbf{x}_i\}, W = \{w_i\})$ is a partition of a domain $\mathcal{D}$ into convex cells $\mathcal{V}_i^w$ such that $\mathcal{V}_i^w = \{\mathbf{x} \in \mathcal{D} \,|\, \|\mathbf{x} - \mathbf{x}_i\|^2 - w_i \leq \|\mathbf{x} - \mathbf{x}_j\|^2 - w_j, \forall j\}$. The dual of power diagram defines the regular triangulation of $(\mathbf{X}, W)$. We denote by $\mathbf{e}_{ij}$ the regular edge between two adjacent points $\mathbf{x}_i$ and $\mathbf{x}_j$, and by $\mathbf{e}_{ij}^*$ the dual (orthogonal and clipped by $\mathcal{D}$) edge separating the partition regions $\mathcal{V}_i^w$ and $\mathcal{V}_j^w$; therefore $\mathbf{x} \in \mathbf{e}_{ij}^*$ iff $\|\mathbf{x} - \mathbf{x}_i\|^2 - w_i = \|\mathbf{x} - \mathbf{x}_j\|^2 - w_j$ and $\mathbf{x} \in \mathcal{D}$. We further indicate by $|\mathbf{e}|$ the length of the edge $\mathbf{e}$ and by Ω_i the one-ring of $\mathbf{x}_i$ in the regular triangulation $(\mathbf{X}, W)$. We also denote by $\mathbf{c}_{ij}$ the intersecting point between the supporting lines of $\mathbf{e}_{ij}$ and $\mathbf{e}_{ij}^*$. As in our main paper, we will refer to the density field in the domain $\mathcal{D}$ as ρ, and denote the average value of ρ over $\mathbf{e}_{ij}^*$ as $\bar{\rho}_{ij}$, and m_i as the integrated value of ρ over $\mathcal{V}_i^w$.

Identities: A few identities involving $\mathbf{c}_{ij}$, directly derived from [Mullen et al. 2011], are important in the rest of this addendum (the $\perp$ symbol refers to counter-clockwise rotation by $90°$):

$$\left\{\begin{array}{l} |\mathbf{e}_{ij}| = d_{ij} + d_{ji} \\[2ex] d_{ij} = \frac{|\mathbf{e}_{ij}|^2 + w_i - w_j}{2|\mathbf{e}_{ij}|} \\[2ex] d_{ji} = \frac{|\mathbf{e}_{ij}|^2 + w_j - w_i}{2|\mathbf{e}_{ij}|} \end{array}\right. \qquad \left\{\begin{array}{l} \mathbf{c}_{ij} = \mathbf{x}_i + \frac{d_{ij}}{|\mathbf{e}_{ij}|}(\mathbf{x}_j - \mathbf{x}_i) \\[2ex] \nabla_{w_i}\mathbf{c}_{ij} \cdot \frac{\mathbf{x}_j - \mathbf{x}_i}{|\mathbf{e}_{ij}|} = \frac{1}{2|\mathbf{e}_{ij}|} \\[2ex] \nabla_{\mathbf{x}_i}\mathbf{c}_{ij} \cdot \frac{\mathbf{x}_j - \mathbf{x}_i}{|\mathbf{e}_{ij}|} = \frac{d_{ij}}{|\mathbf{e}_{ij}|}\frac{\mathbf{x}_j - \mathbf{x}_i}{|\mathbf{e}_{ij}|} \end{array}\right. \qquad \left\{\begin{array}{l} \forall \mathbf{x} \in \mathbf{e}_{ij}^*, \exists t \in \mathbb{R} \text{ s.t. :} \\[2ex] \mathbf{x} = \mathbf{c}_{ij} + t\,(\mathbf{x}_j - \mathbf{x}_i)^\perp \\[2ex] \nabla_{w_i}\mathbf{x} \cdot \frac{\mathbf{x}_j - \mathbf{x}_i}{|\mathbf{e}_{ij}|} = \nabla_{w_i}\mathbf{c}_{ij} \cdot \frac{\mathbf{x}_j - \mathbf{x}_i}{|\mathbf{e}_{ij}|} \end{array}\right.$$

Reynolds' transport theorem: The derivations we present below can be found through Reynolds theorem, which states that the rate of change of the integral of a scalar function f within a volume V is equal to the volume integral of the change of f, plus the boundary integral of the rate at which f flows through the boundary ∂V of outward unit normal $\mathbf{n}$; i.e., in terse notation:

$$\nabla\left(\int_V f(\mathbf{x})\, dV\right) = \int_V \nabla f(\mathbf{x})\, dV + \int_{\partial V} f(\mathbf{x})\, (\nabla\mathbf{x} \cdot \mathbf{n})\, dA.$$

Derivative of m_i: For a fixed domain $\mathcal{D}$, we know that the partition of ρ into cells $\mathcal{V}_i^w$ sums up to a constant, i.e., $\sum_i m_i = $ constant. Consequently:

$$\left\{\begin{array}{l} \nabla_{w_i} m_i + \sum_{j\in\Omega_i} \nabla_{w_i} m_j = 0 \\[2ex] \nabla_{\mathbf{x}_i} m_i + \sum_{j\in\Omega_i} \nabla_{\mathbf{x}_i} m_j = 0 \end{array}\right.$$

We now apply Reynolds theorem to show that the derivative of m_j with respect to w_i is:

$$\boxed{\nabla_{w_i} m_j = -\frac{\bar{\rho}_{ij}}{2}\frac{|\mathbf{e}_{ij}^*|}{|\mathbf{e}_{ij}|}}$$

Proof.

$$\begin{aligned} \nabla_{w_i} m_j &= \int_{\mathcal{V}_j^w} \underbrace{\nabla_{w_i}\rho(\mathbf{x}) d\mathbf{x}}_{=0} + \sum_{k\in\Omega_j} \int_{\mathbf{e}_{jk}^*} \rho(\mathbf{x}) \underbrace{\left(\nabla_{w_i}\mathbf{x} \cdot \frac{\mathbf{x}_k - \mathbf{x}_j}{|\mathbf{e}_{jk}|}\right)}_{= \nabla_{w_i}\mathbf{c}_{jk} \cdot \frac{\mathbf{x}_k - \mathbf{x}_j}{|\mathbf{e}_{jk}|},\, \forall \mathbf{x} \in \mathbf{e}_{jk}^*} d\mathbf{x} \\ &= \int_{\mathbf{e}_{ij}^*} \rho(\mathbf{x}) \left(\nabla_{w_i}\mathbf{c}_{ij} \cdot \frac{\mathbf{x}_i - \mathbf{x}_j}{|\mathbf{e}_{ij}|}\right) d\mathbf{x} \\ &= \int_{\mathbf{e}_{ij}^*} \rho(\mathbf{x}) \frac{-1}{2|\mathbf{e}_{ij}|} d\mathbf{x} = -\frac{\bar{\rho}_{ij}}{2}\frac{|\mathbf{e}_{ij}^*|}{|\mathbf{e}_{ij}|} \end{aligned}$$

$\square$

Optimal transport: We now define the optimal L_2 transport cost between a point $\mathbf{x}_i$ and its dual cell $\mathcal{V}_i^w$:

$$\mathcal{E}_i(\mathbf{X}, W) = \int\limits_{\mathcal{V}_i^w} \rho(\mathbf{x}) \|\mathbf{x} - \mathbf{x}_i\|^2 d\mathbf{x}.$$

The total cost to transport ρ to the points $\mathbf{X}$ is then defined simply as $\mathcal{E}(\mathbf{X}, W) = \sum_i \mathcal{E}_i(\mathbf{X}, W)$.

A direct application of Reynolds theorem leads to the derivatives of $\mathcal{E}$:

$$\boxed{\begin{aligned} &\nabla_{w_i} \mathcal{E}(\mathbf{X}, W) = \sum_{j \in \Omega_i} (w_j - w_i) \nabla_{w_i} m_j \\ &\nabla_{\mathbf{x}_i} \mathcal{E}(\mathbf{X}, W) = 2 m_i (\mathbf{x}_i - \mathbf{b}_i) + \sum_{j \in \Omega_i} (w_j - w_i) \nabla_{\mathbf{x}_i} m_j \end{aligned}}$$

where

$$\mathbf{b}_i = \frac{1}{m_i} \int\limits_{\mathcal{V}_i^w} \mathbf{x} \rho(\mathbf{x}) d\mathbf{x}.$$

Proof. First let's derive the expression for $\nabla_{\mathbf{x}_i} \mathcal{E}$.

$$\begin{aligned} \nabla_{\mathbf{x}_i} \mathcal{E}(\mathbf{X}, W) = & \int\limits_{\mathcal{V}_i^w} \nabla_{\mathbf{x}_i} \left(\rho(\mathbf{x}) \|\mathbf{x} - \mathbf{x}_i\|^2 \right) d\mathbf{x} + \sum_{j \in (\{i\} \cup \Omega_i)} \int\limits_{\partial \mathcal{V}_j^w} \rho(\mathbf{x}) \|\mathbf{x} - \mathbf{x}_j\|^2 \left(\nabla_{\mathbf{x}_i} \mathbf{x} \cdot \mathbf{n} \right) d\mathbf{x} \\ = & \; 2 m_i (\mathbf{x}_i - \mathbf{b}_i) + \sum_{j \in \Omega_i} \int\limits_{\mathbf{e}_{ij}^*} \rho(\mathbf{x}) \underbrace{\left(\|\mathbf{x} - \mathbf{x}_j\|^2 - \|\mathbf{x} - \mathbf{x}_i\|^2 \right)}_{= w_j - w_i, \, \forall \, \mathbf{x} \in \mathbf{e}_{ij}^*} \left(\nabla_{\mathbf{x}_i} \mathbf{c}_{ij} \cdot \tfrac{\mathbf{x}_i - \mathbf{x}_j}{|\mathbf{e}_{ij}|} \right) d\mathbf{x} \\ = & \; 2 m_i (\mathbf{x}_i - \mathbf{b}_i) + \sum_{j \in \Omega_i} (w_j - w_i) \left(\tfrac{d_{ij}}{|\mathbf{e}_{ij}|^2} (\mathbf{x}_i - \mathbf{x}_j) \int\limits_{\mathbf{e}_{ij}^*} \rho(\mathbf{x}) d\mathbf{x} \right) \\ = & \; 2 m_i (\mathbf{x}_i - \mathbf{b}_i) + \sum_{j \in \Omega_i} (w_j - w_i) \nabla_{\mathbf{x}_i} m_j. \end{aligned}$$

The proof for $\nabla_{w_i} \mathcal{E}$ is similar, with the exception that the first term of Reynolds theorem is zero. □

Functional $\mathcal{F}$: In our work we use the extremization of a functional $\mathcal{F}$ which is defined as:

$$\boxed{\mathcal{F}(\mathbf{X}, W) = \mathcal{E}(\mathbf{X}, W) - \sum_i w_i (m_i - m).}$$

By combining the expressions shown so far, we can easily compute the derivatives of $\mathcal{F}$:

$$\boxed{\begin{aligned} &\nabla_{w_i} \mathcal{F}(\mathbf{X}, W) = m - m_i \\ &\nabla_{\mathbf{x}_i} \mathcal{F}(\mathbf{X}, W) = 2 m_i (\mathbf{x}_i - \mathbf{b}_i) \\ &\nabla_w^2 \mathcal{F}(\mathbf{X}, W) = -\Delta^{w, \rho} \end{aligned}}$$

Proof. Based on the expressions derived previously, let's start proving the first-order derivatives:

$$\begin{cases} \nabla_{w_i} \mathcal{F}(\mathbf{X}, W) = \nabla_{w_i} \mathcal{E}(\mathbf{X}, W) - (m_i - m) - \sum_{j \in \Omega_i} (w_j - w_i) \nabla_{w_i} m_j = m - m_i. \\ \nabla_{\mathbf{x}_i} \mathcal{F}(\mathbf{X}, W) = \nabla_{\mathbf{x}_i} \mathcal{E}(\mathbf{X}, W) - \sum_{j \in \Omega_i} (w_j - w_i) \nabla_{\mathbf{x}_i} m_j = 2 m_i (\mathbf{x}_i - \mathbf{b}_i) \end{cases}$$

The second-order derivative with respect to weights is trivial since we know $\nabla_{w_i} m_i$ and $\nabla_{w_i} m_j$. □

Equivalence of Optimizations: We now review the constrained minimization problem presented in the main text and prove more thoroughly the equivalence of solutions to the extremization of our functional $\mathcal{F}$ and the extremization of the Lagrangian $\mathcal{L}$.

First we define our constrained minimization problem as:

$$\boxed{\min \mathcal{E}(\mathbf{X}, W) \quad \text{s.t.} \quad m_i = m \quad \forall i.}$$

With Lagrangian multipliers $\Lambda = \{\lambda_i\}$ we can solve such problem by extremizing the Lagrangian:

$$\mathcal{L}(\mathbf{X}, W, \Lambda) = \mathcal{E}(\mathbf{X}, W) + \sum_i \lambda_i (m_i - m).$$

Therefore, for any extremum $(\mathbf{X}^*, W^*, \Lambda^*)$ of $\mathcal{L}$ the following conditions hold:

$$\begin{cases} 0 = \nabla_{w_i} \mathcal{L}(\mathbf{X}^*, W^*, \Lambda^*) = \nabla_{w_i} \mathcal{E}(\mathbf{X}^*, W^*) + \sum_{j \in \Omega_i} (\lambda_j^* - \lambda_i^*) \nabla_{w_i} m_j \\ 0 = \nabla_{\mathbf{x}_i} \mathcal{L}(\mathbf{X}^*, W^*, \Lambda^*) = \nabla_{\mathbf{x}_i} \mathcal{E}(\mathbf{X}^*, W^*) + \sum_{j \in \Omega_i} (\lambda_j^* - \lambda_i^*) \nabla_{\mathbf{x}_i} m_j \\ 0 = \nabla_{\lambda_i} \mathcal{L}(\mathbf{X}^*, W^*, \Lambda^*) = m_i - m \end{cases}$$

Note that the first condition reduces simply to $\Delta^{w,\rho}(\Lambda^* + W^*) = 0$, and thus $\Lambda^* = \text{constant} - W^*$. By replacing the Lagrangian multipliers Λ^* with the negated weights W^*, we conclude that $\nabla_{\mathbf{x}_i} \mathcal{L}(\mathbf{X}^*, W^*, \Lambda^*) = 2m_i(\mathbf{x}_i^* - \mathbf{b}_i) = 0$. Hence, any extremum of $\mathcal{L}$ is also an extremum of $\mathcal{F}$ and vice-versa.

2 More Results

The following images are additional results of our algorithm, obtained automatically without parameter tuning. First, we show in Fig. 1 blue noise point sets before and after our regularity breaking procedure (from Fig. 5 in our paper), with a color for each point indicating the weight values optimized. Fig. 2 then shows the blue noise point distribution of an image generated by our method compared to the recent approach of [Chen et al. 2012]. We show two other stippling examples, in Fig. 3 and Fig. 4. We also present additional comparisons of our method vs. the results of [Schlömer et al. 2011], complementing Fig. 8 of the main text. Finally, we provide large images for the zoneplate tests. Note the presence of second noisy rings in the results obtained by previous methods, contrasting with the anti-aliased reconstruction achieved with our method.

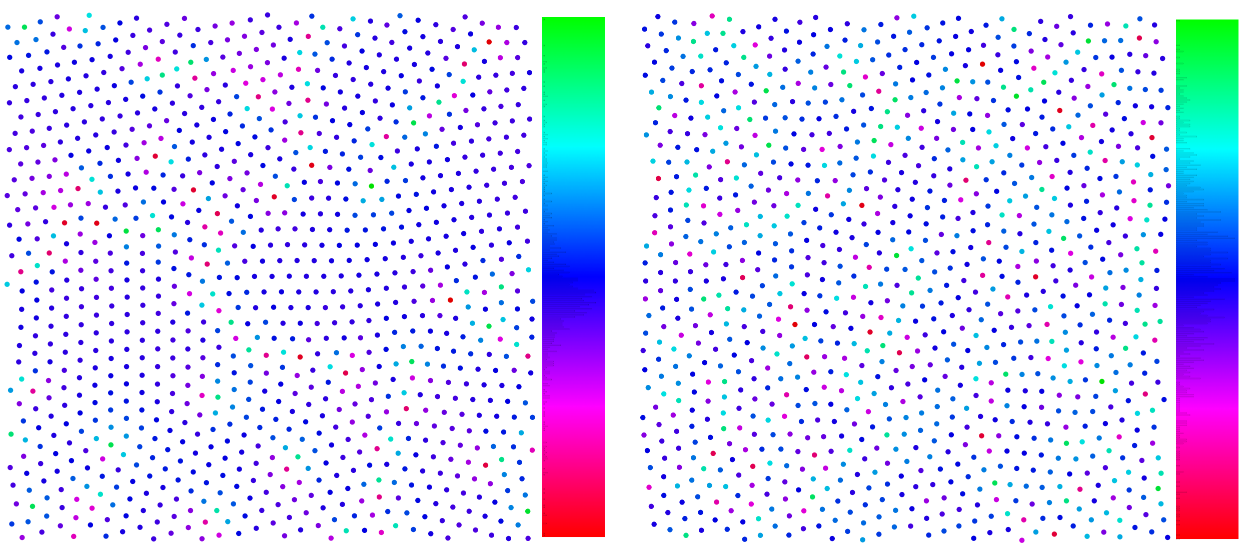

Figure 1: ***Weight Range****: Blue noise distributions before and after breaking regularities on a constant density over a periodic domain (from Fig. 5 in the main paper). Colors of dots indicate weight values (with zero mean), ranging from -4% to 4.5% of the average squared edge length in the regular triangulation. The histogram of the weights is also shown on top of the color ramp.*

References

BALZER, M., SCHLÖMER, T., AND DEUSSEN, O. 2009. Capacity-constrained point distributions: A variant of Lloyd's method. *ACM Trans. Graph. (SIGGRAPH) 28*, 3, 86:1–8.

CHEN, Z., YUAN, Z., CHOI, Y.-K., LIU, L., AND WANG, W. 2012. Variational blue noise sampling. *IEEE Trans. Vis. Comput. Graphics 18*, 10, 1784–1796.

DU, Q., FABER, V., AND GUNZBURGER, M. 1999. Centroidal Voronoi Tessellations: Applications and algorithms. *SIAM Rev. 41* (Dec.), 637–676.

FATTAL, R. 2011. Blue-noise point sampling using kernel density model. *ACM Trans. Graph. (SIGGRAPH) 30*, 3, 48:1–48:12.

MULLEN, P., MEMARI, P., DE GOES, F., AND DESBRUN, M. 2011. HOT: Hodge Optimized Triangulations. *ACM Trans. Graph. (SIGGRAPH) 30*, 3.

SCHLÖMER, T., HECK, D., AND DEUSSEN, O. 2011. Farthest-point optimized point sets with maximized minimum distance. In *Symp. on High Performance Graphics*, 135–142.

XU, Y., LIU, L., GOTSMAN, C., AND GORTLER, S. J. 2011. Capacity-constrained Delaunay triangulation for point distributions. *Comput. Graph. 35*, 510–516.

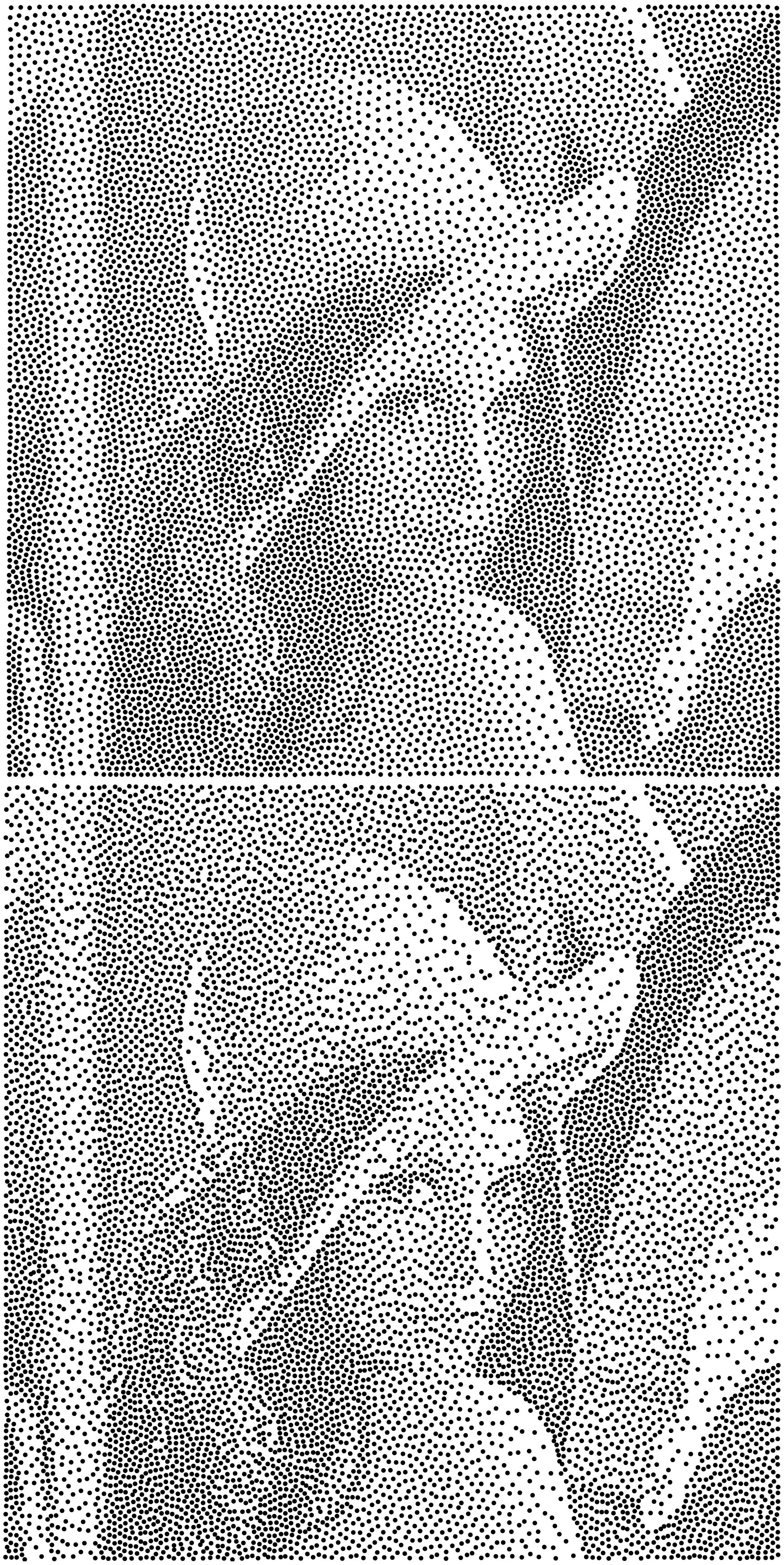

Figure 2: ***Lena****: 10K sites; (top) result generated by our algorithm in 37 seconds (with an Intel Core i7 2.2 GHz laptop, 4GB RAM); (bottom) result of [Chen et al. 2012] (provided by the authors) in 22 seconds (with an Intel Xeon 3.16GHz quad-core, 8GB RAM).*

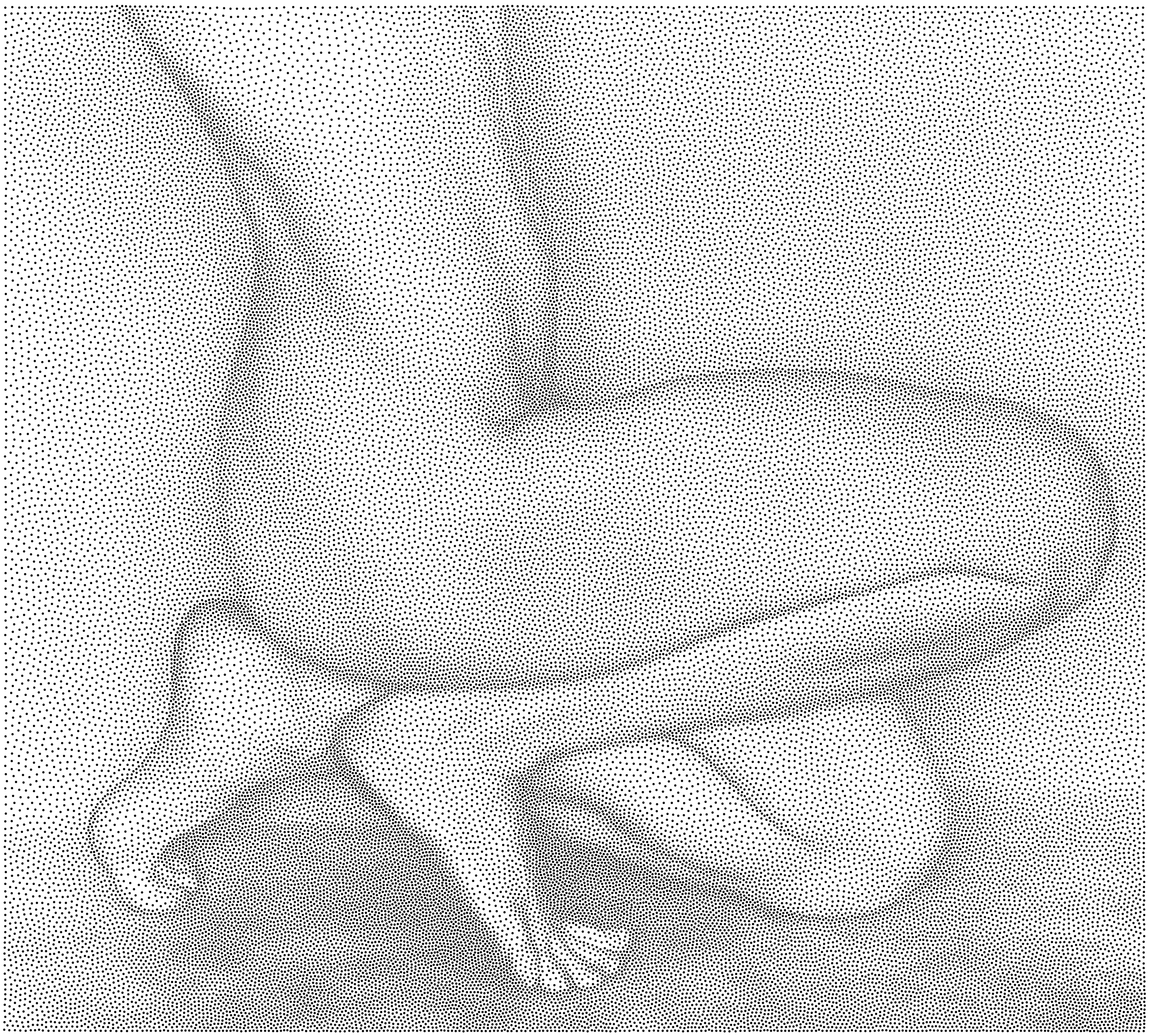

Figure 3: ***Dancer****: 50K sites, 1181x1024 image, 3 mins. From a photograph by Edward Weston.*

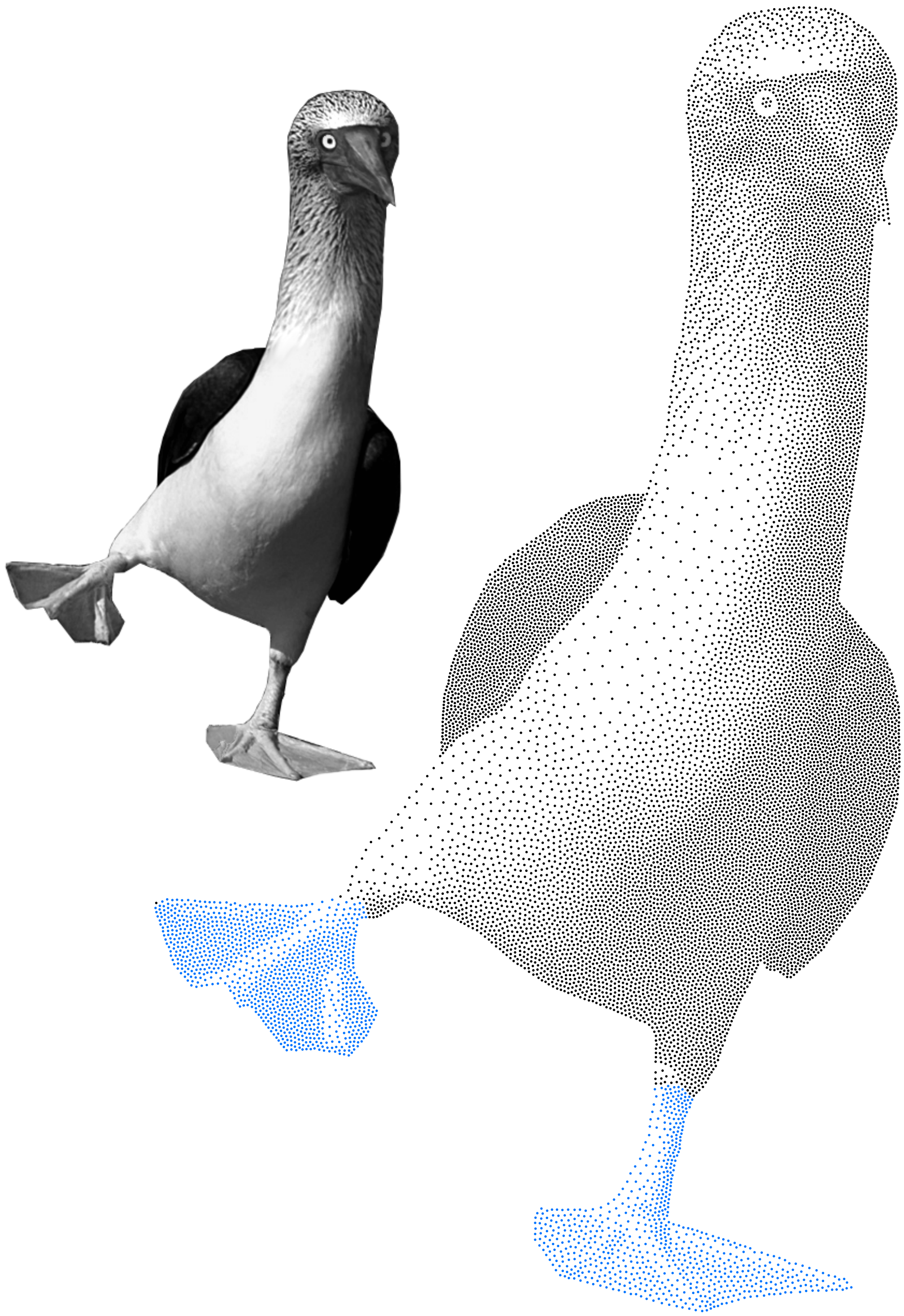

Figure 4: ***Booby Bird.*** *A 376x651 image of a blue-footed booby bird (top left) is sampled with 15K points in 70 seconds with our approach. Note that we post-processed the points on its feet by turning them blue to honor its name.*

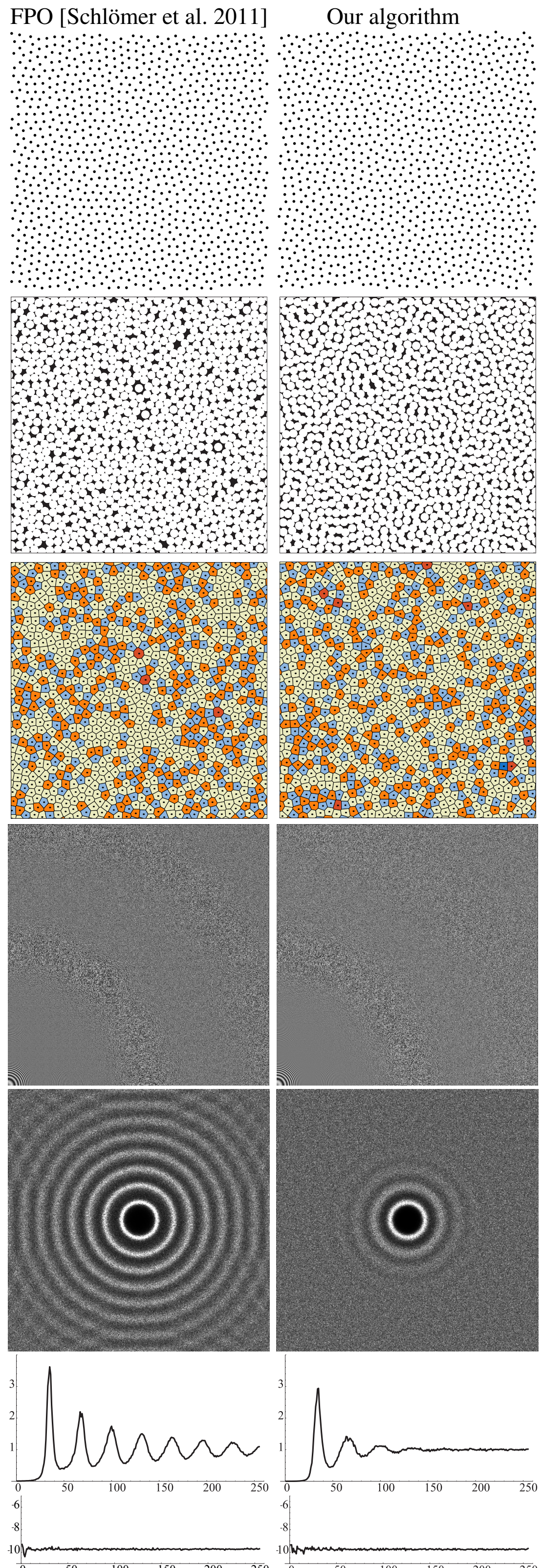

Figure 5: ***More Comparisons.*** *Additional comparison of our results vs. the method of [Schlömer et al. 2011] for a constant density function over a periodic domain, complementing Fig. 8 of the main text.*

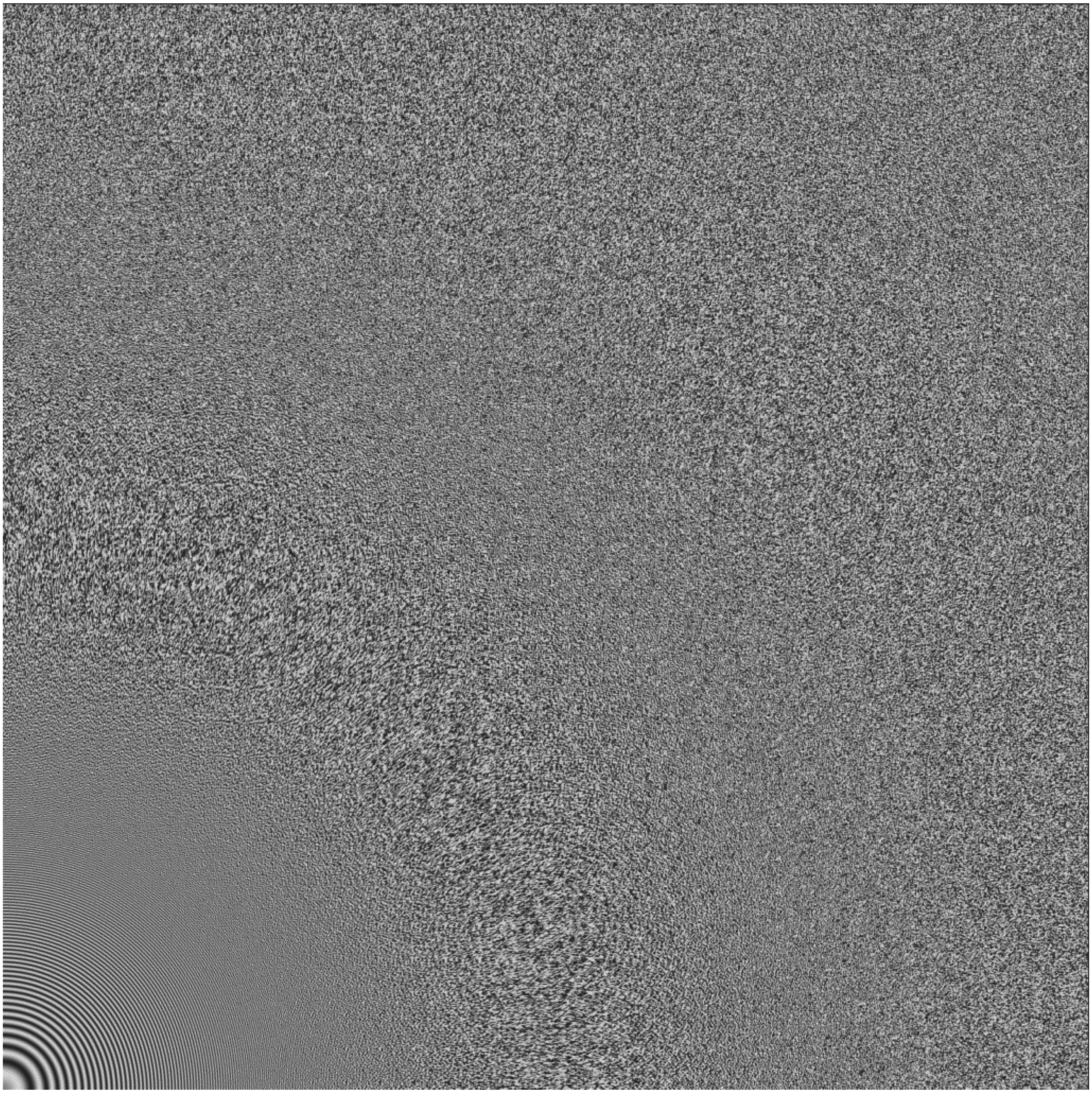

Figure 6: ***Zoneplate for our algorithm.***

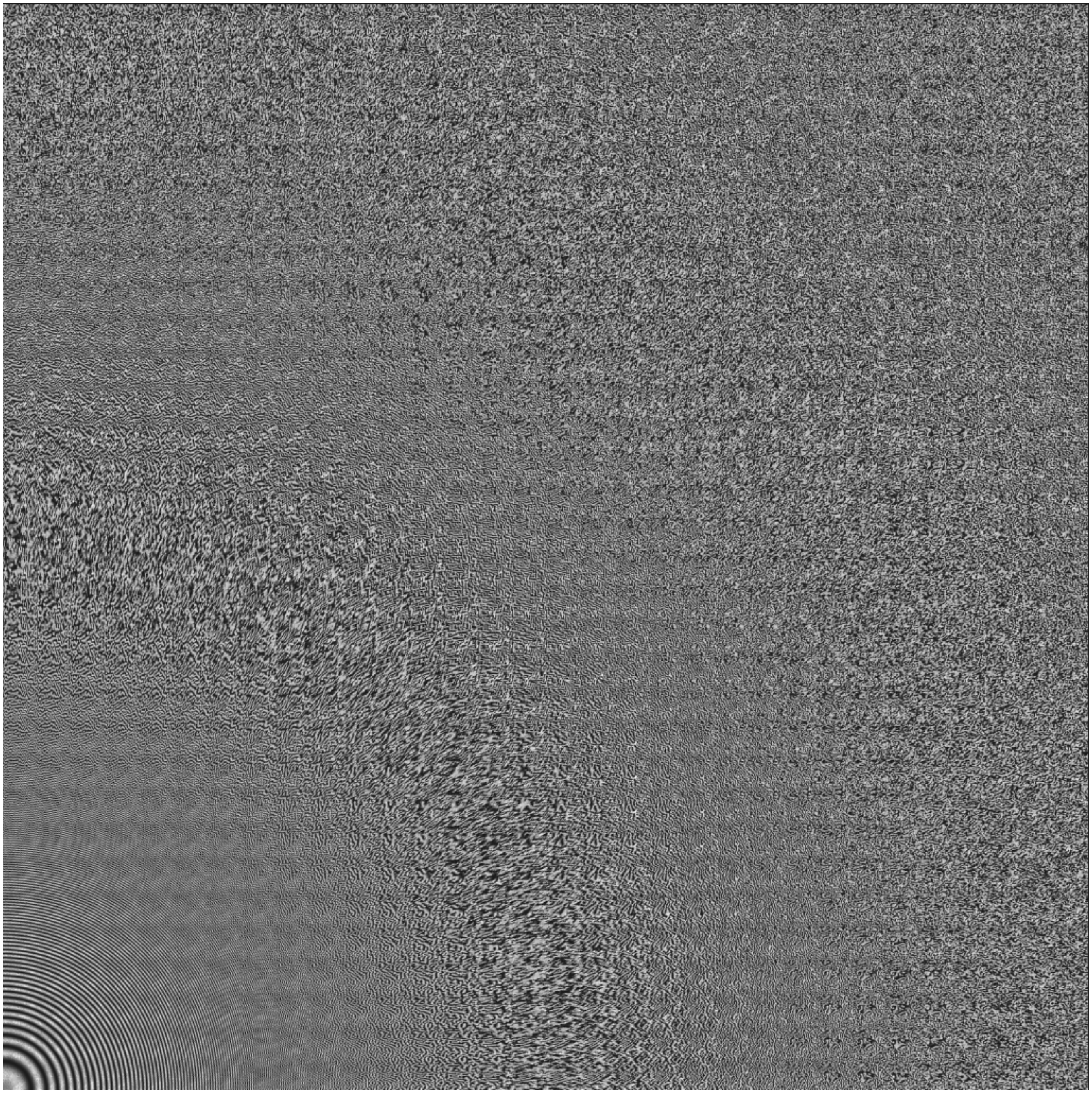

Figure 7: ***Zoneplate for CVT [Du et al. 1999].*** *Stopped at* $\alpha = 0.75$.

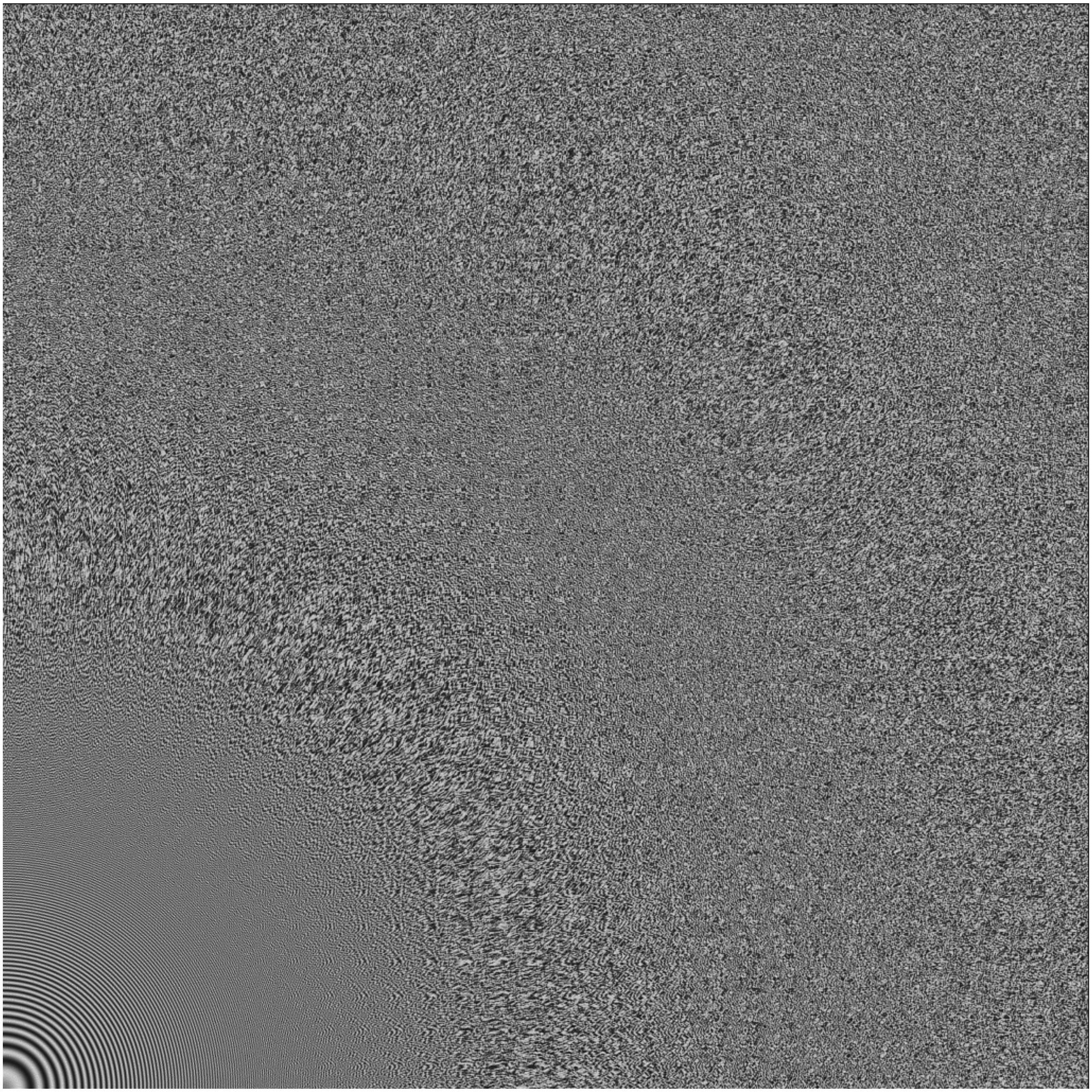

Figure 8: ***Zoneplate for CCDT [Xu et al. 2011].***

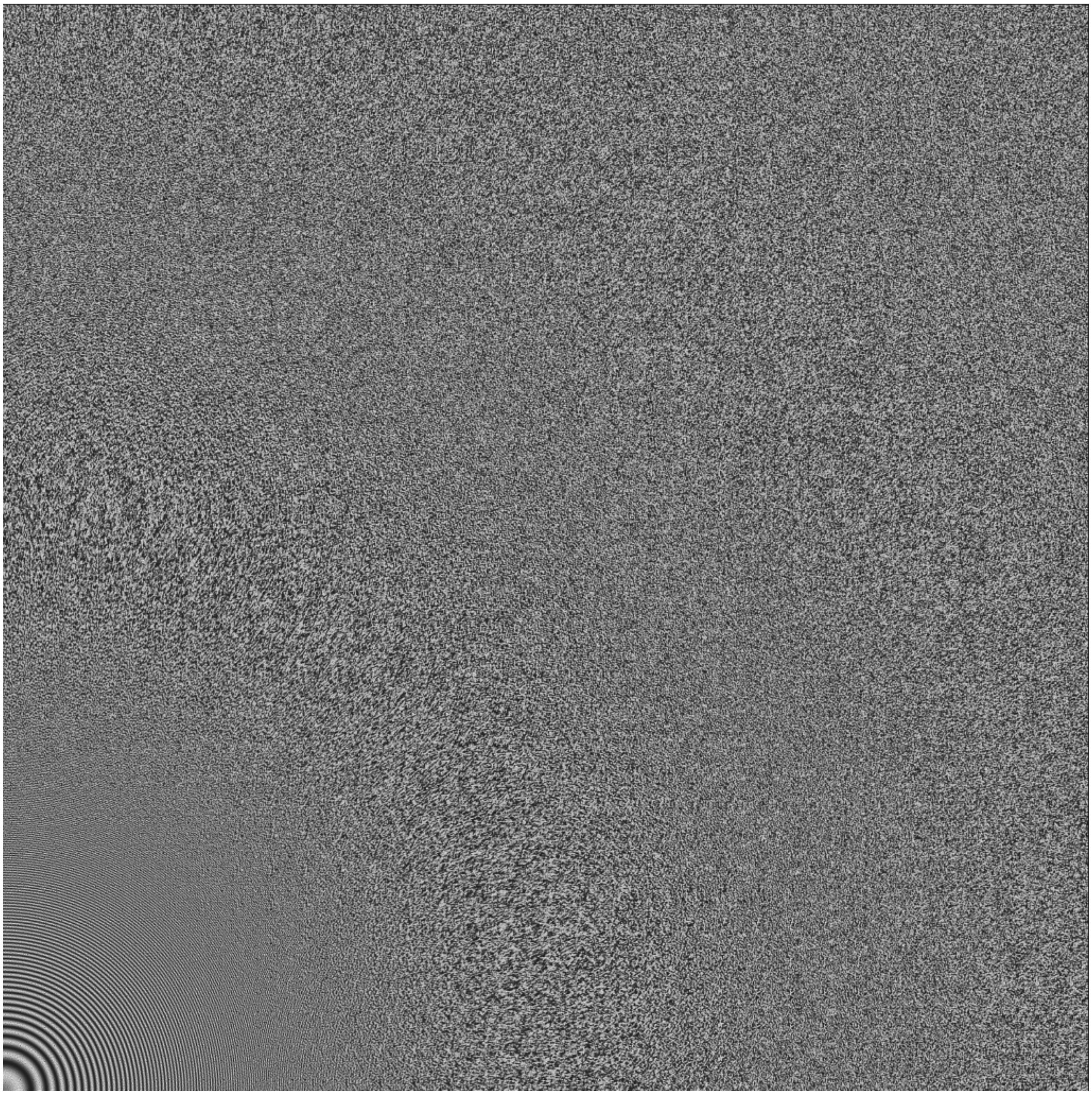

Figure 9: ***Zoneplate for CapCVT [Chen et al. 2012].***

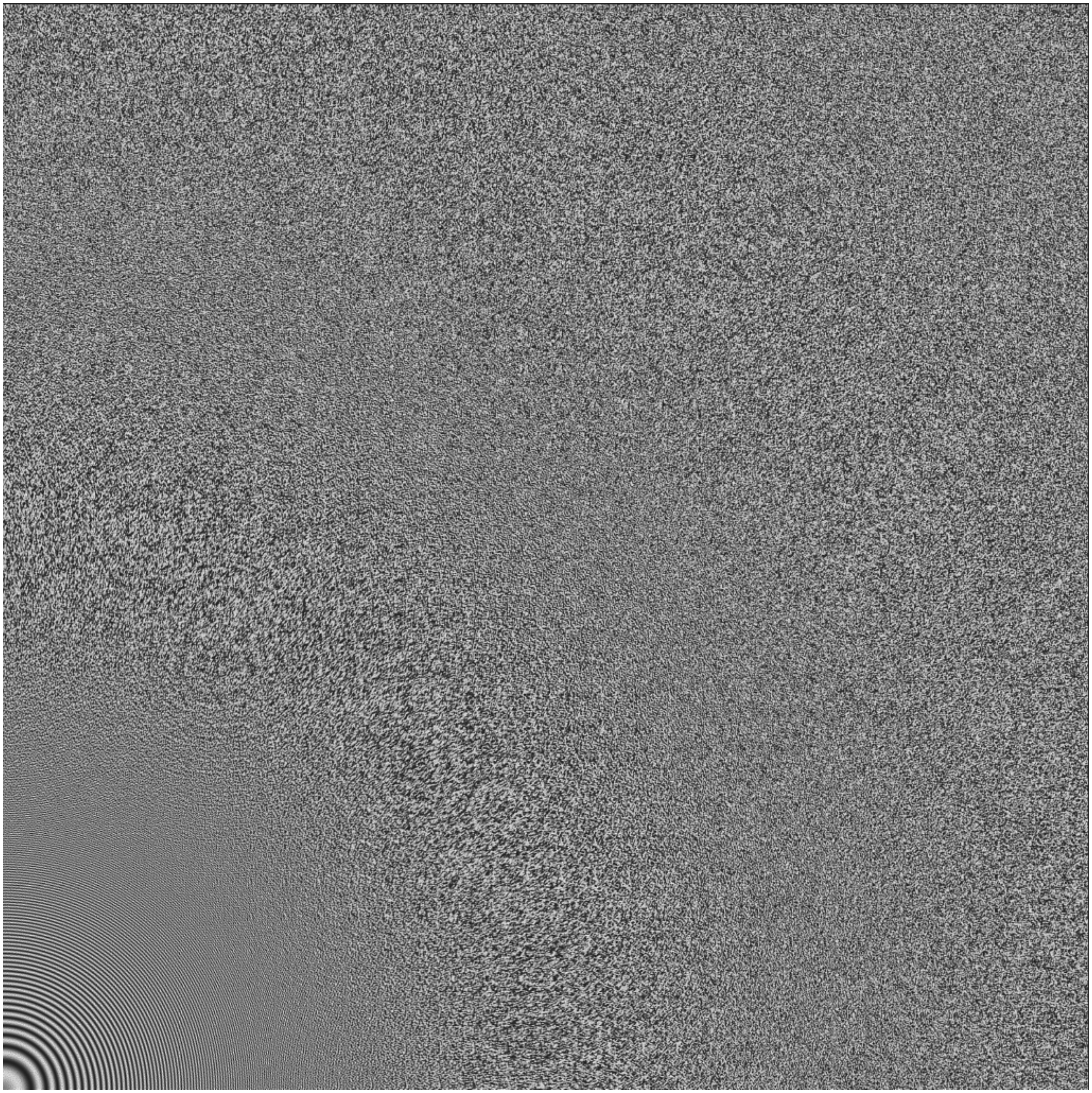

Figure 10: ***Zoneplate for CCVT [Balzer et al. 2009].***

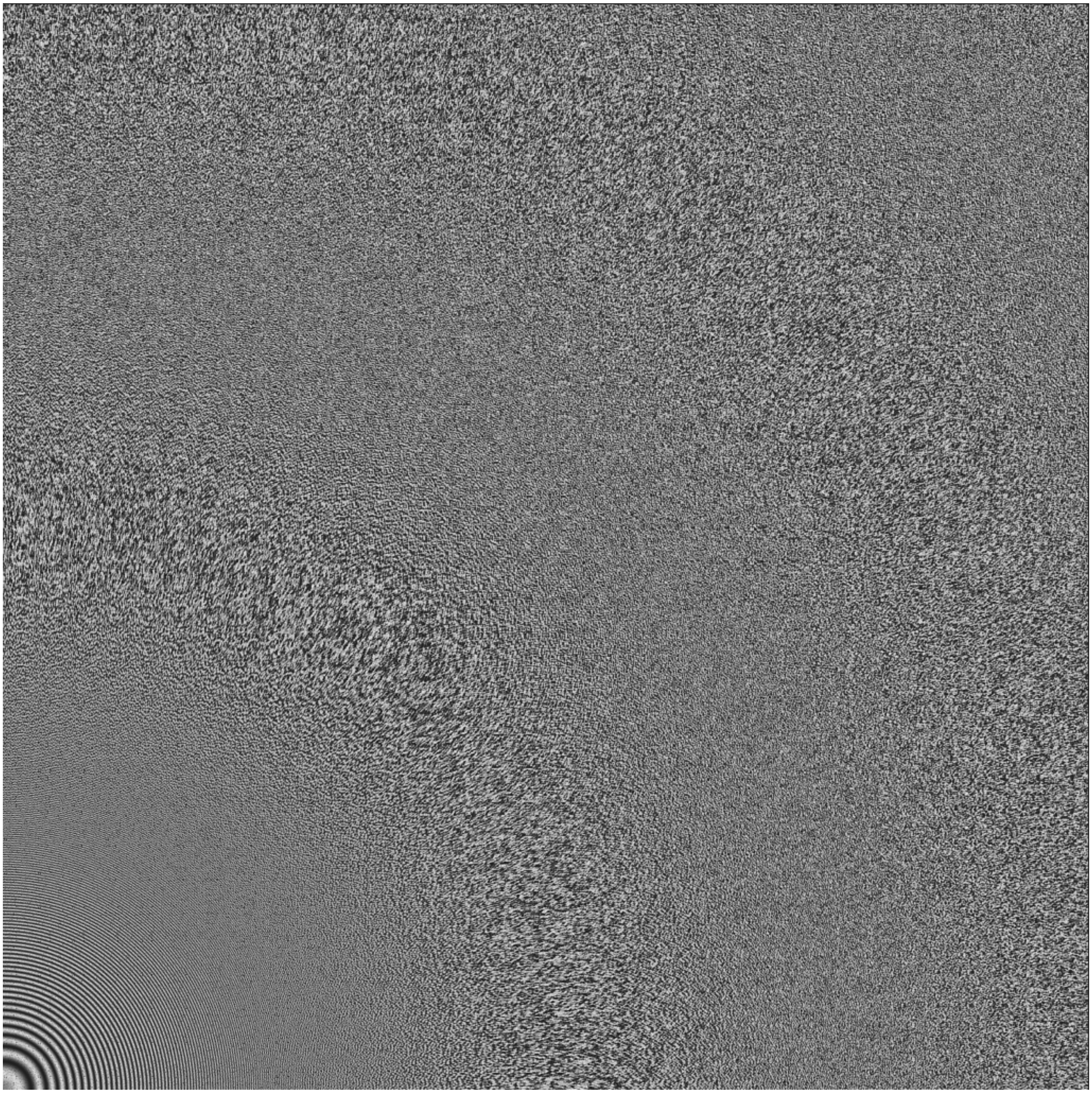

Figure 11: ***Zoneplate for FPO [Schlömer et al. 2011].***

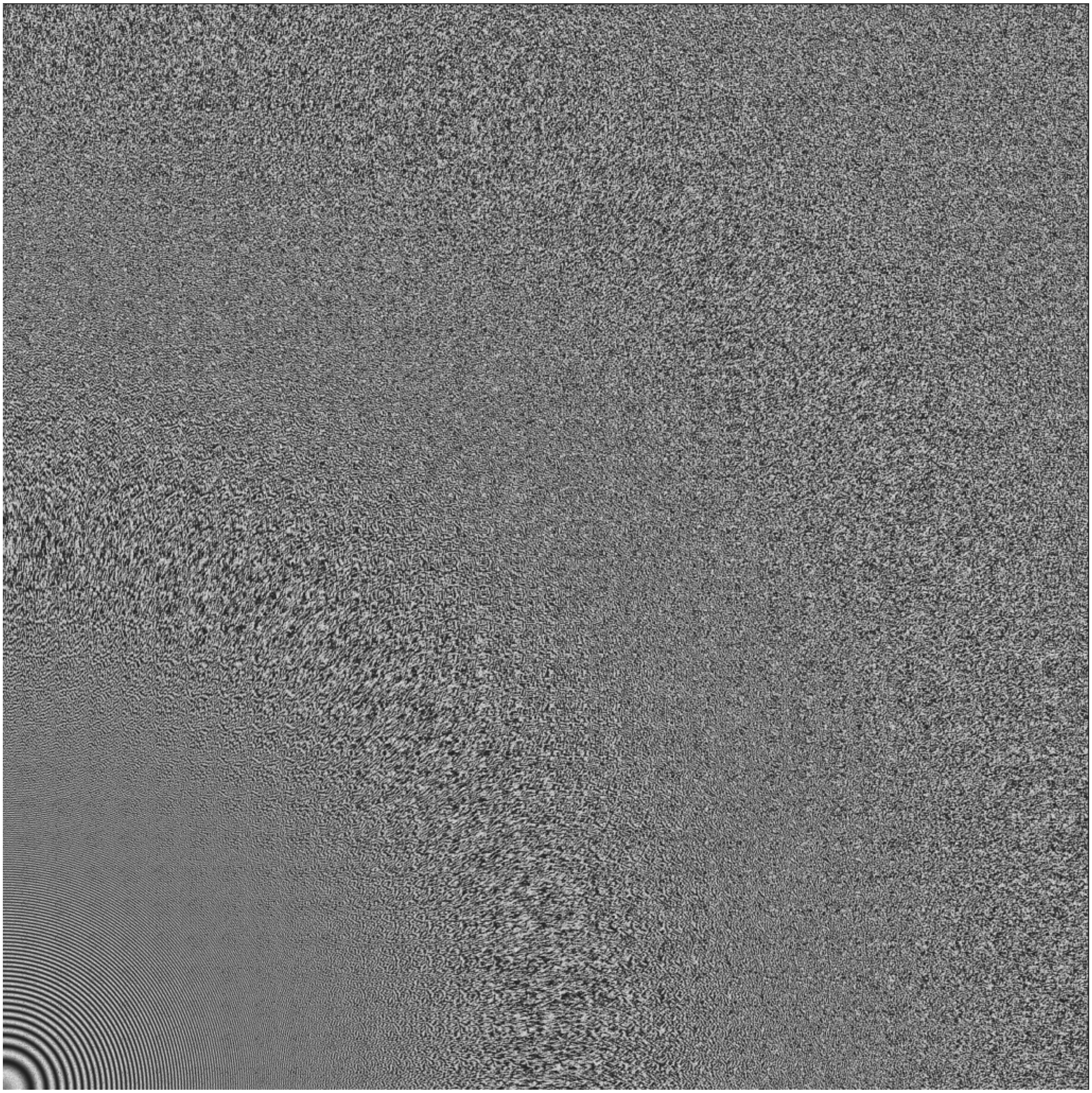

Figure 12: ***Zoneplate for [Fattal 2011].***